International Journal of Applied Earth Observations and Geoinformation 98 (2021) 102310

Contents lists available at ScienceDirect

International Journal of Applied Earth Observations and Geoinformation

journal homepage: www.elsevier.com/locate/jag

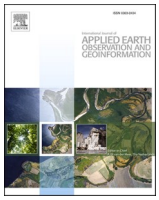

Characterizing forest disturbances across the Argentine Dry Chaco based on Landsat time series

Teresa De Marzo [a,b,*], Dirk Pflugmacher [a], Matthias Baumann [a], Eric F. Lambin [b,d,e], Ignacio Gasparri [c], Tobias Kuemmerle [a]

[a] Geography Department, Humboldt-Universität zu Berlin, Unter den Linden 6, 10099 Berlin, Germany
[b] Georges Lemaître Centre for Earth and Climate Research, Earth and Life Institute, Université catholique de Louvain, 3, place Louis Pasteur, 1348 Louvain-la-Neuve, Belgium
[c] CONICET, Instituto de Ecología Regional (IER), Universidad Nacional de Tucumán, CC:34, CP 4107 Yerba Buena, Tucumán, Argentina
[d] School of Earth, Energy & Environmental Sciences, Stanford University, 473 Via Ortega, Stanford, CA 94305, United States
[e] Woods Institute for the Environment, Stanford University, 473 Via Ortega, Stanford, CA 94305, United States

ARTICLE INFO

Keywords:
Ensemble classification
Forest degradation
LandTrendr
Trajectory analyses
Tropical dry forests
Random Forests

ABSTRACT

Forest loss in the tropics affects large areas, but whereas full forest conversions are routinely assessed, forest degradation patters remain often unclear. This is particularly so for the world's tropical dry forests, where remote sensing of forest disturbances is challenging due to high canopy complexity, strong phenology and climate variability, and diverse degradation drivers. Here, we used the full depth of the Landsat archive and devised an approach to detect disturbances related to forest degradation across the entire Argentine Dry Chaco (about 489,000 km^2) over a 30-year timespan. We used annual time series of different spectral indices, summarized for three seasonal windows, and applied LandTrendr to temporally segment each time series. The resulting pixel-level forest disturbance metrics then served as input for a Random Forests classification which we used to produce an area-wide disturbance map, and associated yearly area estimates of disturbed forest. Finally, we evaluated disturbance trends in relation to climate and soil conditions. Our best model produced a disturbance map with an overall accuracy of 79%, with a balanced error distribution. A total of 8% (24,877 ± 860 km^2) of the remaining forest in the Argentine Dry Chaco have been affected by forest disturbances between 1990 and 2017. Diverse spatial patterns of forest disturbances indicate a variety of agents driving disturbances. We also found the disturbed area to vary strongly between years, with larger areas being disturbed during drought years. Our approach shows that it is possible to robustly map forest disturbances in tropical dry forests using Landsat time series, and demonstrates the value of ensemble approaches to capture spectrally-complex and heterogeneous land-change processes. For the Chaco, a global deforestation hotspot, our analyses provide the first Landsat-based assessment of forest disturbance in remaining forests, highlighting the need to better consider such disturbances in assessments of carbon budgets and biodiversity change.

1. Introduction

Tropical dry forests (TDF) are widespread but typically receive less attention in research and policy-making than moist rainforests (Miles et al., 2006; Schröder et al., 2021). This is unfortunate, as many TDF regions today contain little forest cover due to the historically widespread conversion of forest to agriculture. Where sizable areas of TDF still exist, they are typically under substantial conversion pressure (Miles et al., 2006; Portillo-Quintero and Sánchez-Azofeifa, 2010). Moreover, even those forests that are spared from conversion are under high, and often rising, human influence, as a range of land-use activities lead to forest degradation within them (Sánchez-Azofeifa et al., 2005). These activities include selective logging, fuelwood collection, charcoal production, mining, forest grazing and anthropogenic fires (Miles et al., 2006; Murdiyarso et al., 2007; Sasaki and Putz, 2009; Schneibel et al., 2017). Understanding how such land-use activities contribute to tropical dry forest degradation is therefore important, given the critical ecological state of many TDF.

Forest degradation is the process leading to the permanent deterioration in the density, composition or structure of forest cover (Grainger,

* Corresponding author at: Geography Department, Humboldt-Universität zu Berlin, Unter den Linden 6, 10099 Berlin, Germany.
E-mail address: teresa.demarzo@hu-berlin.de (T. De Marzo).

https://doi.org/10.1016/j.jag.2021.102310
Received 24 September 2020; Received in revised form 13 January 2021; Accepted 31 January 2021
Available online 19 February 2021

1993). These changes can have widespread and major impacts on ecosystem functioning, biodiversity and ecosystem services (Watson et al., 2018). For instance, degraded forests store and sequester less carbon (Pan et al., 2011) and sustain less biodiversity (Betts et al., 2017; Gibson et al., 2011) than undegraded forests, and forest degradation might threaten indigenous communities that depend on intact forests (Rozzi, 2012). Monitoring forest condition and uncovering drivers of forest degradation is therefore important to understand the wider social-ecological implications of degradation, particularly considering that degradation is a widespread phenomenon in the tropics (Asner et al., 2005; Pearson et al., 2017). Having accurate estimates of forest degradation is furthermore needed to inform and implement global and national climate mitigation initiatives, such as the United Nation's (UN) Reducing Emissions from Deforestation and Forest Degradation (REDD+) programme (Goetz et al., 2015). Nonetheless, we still lack robust information on the extent of degraded forests, mainly due to the conceptual and technical challenges related to detecting and mapping degradation (Da Ponte et al., 2015; Sasaki and Putz, 2009).

Degradation is typically assumed to be caused by an increase in anthropogenic disturbance (Lambin, 1999). A wide range of land-use activities that disturb forest structure and biomass can lead to declining productivity, canopy cover and stand complexity (Grainger, 1993). An important step to understand forest degradation is therefore the reliable monitoring of disturbances in forest canopies that are the result of degradation drivers, such as selective logging or anthropogenic fires (Hethcoat et al., 2019; Hirschmugl et al., 2014; Matricardi et al., 2010; Souza et al., 2005). Detecting such canopy disturbances in tropical forests with remote sensing can be challenging though, as disturbances have diverse impacts on forest structure, leave varying tree cover, and occur in diverse patch sizes, ranging from individual trees taken out to large forest fires. Moreover, some disturbances disappear quickly as forests recover, while others last for a long time (Hirschmugl et al., 2014). Because many forest disturbances associated with forest degradation result in subtle and gradual canopy changes, they can easily be confused with phenology or natural fluctuations in forest condition, for instance due to varying rainfall (Cohen et al., 2010; Lambin, 1999). The latter is particularly important for TDF regions, which experience marked interannual climate variability (Murphy and Lugo, 1986). Robust monitoring of forest degradation in TDF therefore requires appropriate methodologies to deal with this complexity, but such methodologies are overall missing. This translates into a paucity of knowledge on degradation trends in TDF (Morales-Barquero et al., 2015; Sánchez-Azofeifa et al., 2005; Sánchez-Azofeifa and Portillo-Quintero, 2011).

Analysing long time series of images can provide a quasi-continuous history of forest disturbance and regeneration (Da Ponte et al., 2015). Such long, decadal time series are thus potentially well-suited to capture forest degradation trends. With its open data policy and long time span, the Landsat archive provides time series at spatial resolution fine enough to monitor forest degradation (Woodcock et al., 2020). In addition, many algorithms have been developed to automatize forest-disturbance assessments, such as the Landsat-based detection of Trends in Disturbance and Recovery (LandTrendr; Kennedy et al., 2010), the Breaks for Additive Season and Trend (BFAST; Verbesselt et al., 2010), the Continuous Change Detection and Classification (CCDC; Zhu and Woodcock, 2014), or the Vegetation Regeneration and Disturbance Estimates through Time (VeRDET; Hughes et al., 2017) algorithms. Application of these algorithms has recently also moved from using time series of individual indices (e.g., band 5, NDVI, NBR) towards employing ensembles approaches that have considerable potential for capturing disturbances (Bullock et al., 2019; Cohen et al., 2018; Healey et al., 2018; Schultz et al., 2016). Two types of ensemble approaches have been tested: spectral ensemble approaches, where individual disturbance-detection runs are done for different spectral bands or indices using one algorithm, and then a classifier derives the final disturbance product (Cohen et al., 2018; Wang et al., 2019), or an algorithm ensemble approach, where the output from multiple disturbance-detection algorithms is used to feed the classification (Healey et al., 2018; Hislop et al., 2019; Saxena et al., 2018). While these studies show that ensemble techniques can produce more accurate forest disturbance maps, such approaches have not been tested to map disturbances and forest degradation for a large TDF area.

One TDF region where trends and patterns of forest degradation remain poorly understood is the South American Gran Chaco. Here, alongside the massive and relatively well-understood conversion of forest to agriculture that has happened since the 1990s (Baumann et al., 2017; Gasparri and Grau, 2009; Grau et al., 2005; Piquer-Rodríguez et al., 2018), a variety of land uses inside remaining forests cause forest degradation (Adamoli et al., 1990; Bachmann et al., 2007; Bucher and Huszar, 1999; Cabido et al., 2018; Grau et al., 2008; Torrella and Adámoli, 2005). However, the extent, severity, and timing of forest disturbances potentially associated with degradation have never been quantified for larger regions in the Chaco. Better information about the broad-scale patterns of forest condition would be important, as forests continue to be lost at alarming rates.

Focussing on the entire Argentine Dry Chaco (489,000 km^2), our goal was to identify rates and patterns of forest disturbances in remaining Chaco forests. Specifically, our objectives were to:

1. assess the usefulness of a range of Landsat-based spectral indices and time periods over which metrics are calculated to capture forest disturbances in TDF.
2. map forest disturbances potentially related to forest degradation across the entire Argentine Dry Chaco.
3. assess the extent and spatiotemporal patterns of forest disturbance across the Dry Chaco, generally and in relation to rainfall and soil patterns.

2. Study area

The Gran Chaco is the largest remaining continuous tropical dry forest of the world (Olson et al., 2001). We focus on 489,000 km^2 study area in the Dry Chaco in northern Argentina, which was covered by about 370,000 km^2 of forest at the beginning of our study period in 1987. Climate in the Dry Chaco is strongly seasonal, with a distinct dry season between May and September, and a hot, rainy season from November to April. Annual rainfall ranges from 1,200 mm in the east to 450 mm in the west and the average temperature is around 22 °C (Minetti, 1999). The area is characterized by flat terrain, except for the west and southwest where hilly terrain prevails. Vegetation consists of a mosaic of xerophytic forests, open woodlands, scrubs, savannas and grasslands. Characteristic tree species belong to the generum *Schinopsis*, in particular *S. balansae* ("Quebracho colorado chaqueño"), *S. quebracho-colorado* ("Quebracho colorado"), *S. hankeana* ("Horco quebracho"). Also forests of *Bulnesia sarmentoi* ("Palo santo") are characteristic and those dominated by *Aspidosperma quebracho-blanco* ("Quebracho blanco"). Trees of Prosopis spp. ("Algarrobos") are also very common. The shrub layer is dominated by species of the genus *Acacia*, *Mimosa*, *Prosopis*, *Celtis*, and cacti *Opuntia* and *Cereus*. Some savannas are also present, dominated by grasses *Elionorus muticus* or *Spartina argentinensis*, and palm savannas of *Copernicia alba*. (Bucher, 1982; Cabido et al., 2018; Prado, 1993).

During the last decades, the Chaco experienced dramatic forest loss caused by agricultural expansion (Fehlenberg et al., 2017; Gasparri and Grau, 2009). In addition, several land-use activities lead to forest degradation. Logging, charcoal production, fires and overgrazing are the main drivers of degradation. Logging can be related to the production of firewood, fence poles, tannin or charcoal (Bachmann et al., 2007; Rueda et al., 2015), typically leading to the extraction of large trees (e.g., *Schinopsis lorentzii* and *Aspidosperma quebracho-blanco*). Because logging historically has often been unsustainable, a simplification of forest structure and composition, and a shift to shrub-dominated communities

has happened in many places in the Chaco (Torrella and Adámoli, 2005). Fire, although a natural and ecologically important disturbance agent in the region (Adamoli et al., 1990), is another key driver of forest degradation (Bachmann et al., 2007). Fire is used to promote the regrowth of grasses on pastures, to burn waste on fields, and to convert forest into agricultural land (Bachmann et al., 2007). In all these cases, fires can escape to nearby forest, causing degradation. Likewise, fire is often used as a management tool to clear the shrub layer and to facilitate the extraction of partly burnt trees for fuelwood and charcoal (Zak et al., 2004). Finally, forest grazing exerts considerable pressure on forest in the Chaco. Forest grazing is a traditional management practice related to small-scale cattle ranching that largely affects the forest (Grau et al., 2008; Macchi and Grau, 2012). Grazing pressure alters the herbaceous/woody vegetation dynamic by favouring shrubs (Adamoli et al., 1990) leading to the virtual elimination of grasses and a dominance of shrubs and small trees (Torrella and Adámoli, 2005).

3. Data and methods

Our methodology consisted of four main steps (Fig. 1). In step 1, we built annual time series of Landsat-derived indices to which we then, in step 2, applied temporal segmentation to extract disturbance metrics per pixel. In a third step, we used a random forests classifier, trained with an extensive reference dataset, to map disturbances for each spectral index, as well as for the ensemble of all indices. In our final and fourth step, we used the best-performing model and associated disturbance map to estimate yearly disturbed areas using an unbiased estimator based on an independent set of reference points.

3.1. Annual composites of spectral indices

In the first step, we derived consistent time series of a range of spectral-temporal metrics based on all available Landsat imagery. To do that, we collected all available Landsat TM, ETM+ and OLI images for the period 1987–2017 as Collection 1 Tier 1 surface reflectance data in Google Earth Engine. These data are atmospherically corrected, have the lowest geo-registration errors and come with a pixel Quality Assessment (QA) band based on CFMask (Foga et al., 2017). We masked out all clouds and cloud shadows using the respective QA band values and applied the coefficients by Roy et al. (2016) for cross-calibration of SR-values between OLI and ETM+ data. We also calculated a set of spectral indices, specifically the Tasselled Cap Wetness (TCW, Kauth and Thomas, 1976), the Normalized Burn Ratio (NBR, Key and Benson, 1999), and the Normalized Difference Moisture Index (NDMI, Gao, 1996). We then subdivided for each year of our study period the yearly image collection into three seasonal image collections (February-April, May-July, August-October), and calculated for each period the medoid (Flood, 2013) of our spectral indices. The choice of these intervals resulted from consideration about the phenology of our system: we targeted the beginning of the dry season (May-July) because this is the time when herbaceous vegetation is dry, but trees have not shed their leaves yet. However, this period is also phenologically dynamic, which makes trend analyses more sensitive to false disturbance detections, depending on data availability. Therefore, we decided to also test the interval before and after (February-April and August-October) when vegetation phenology is relatively stable. This resulted in a set of 9 annual medoid time stacks (i.e., 3 indices × 3 seasons), which served as input for the LandTrendr segmentation. We masked all index stacks to exclude areas that had not been forest in our study period using a forest mask from the onset of our study period (Baumann et al., 2017).

3.2. Disturbance metrics

We then applied LandTrendr, as implemented in Google Earth Engine, to each of our nine stacks (Kennedy et al., 2018). LandTrendr is a temporal segmentation algorithm that fits spectral trajectories on a pixel-per-pixel basis, using regression methods and point-to-point fitting across the annual time series of values (Kennedy et al., 2010). LandTrendr works by iteratively identifying a set of vertices and then fitting linear segments between them in order to obtain a continuous trajectory

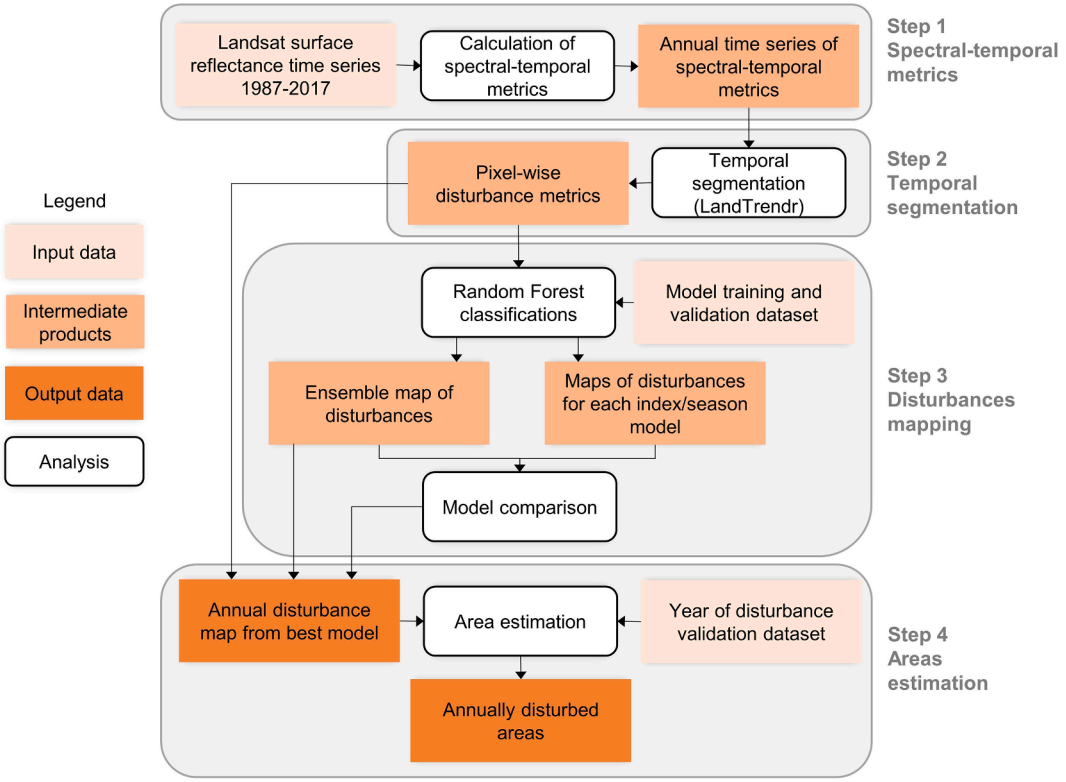

Fig. 1. Workflow of our analysis to map disturbances related to degradation in the tropical dry forest of the Argentine Gran Chaco.

through the time series (see Kennedy et al., 2010 for details). The result of this procedure is a simplified, piece-wise representation of the annual time series. Based on these time series, a number of metrics can be derived, such as the number and length (in years) of segments, their slope, and the years corresponding to segment vertices.

LandTrendr requires tuning several parameters (Table 1). We did this by visually inspecting samples at exemplary regions where key disturbance processes, including selective logging and fire, were known to occur. These exemplary regions were derived from the literature, pointed out by local experts (including co-authors with 10+ years of field experience in the Chaco) or identified on very high-resolution images on Google Earth. We visually evaluated how different parameters changed the trajectory fitting for these exemplary regions, and chose the parameter combination that across samples visually resulted in the best time series segmentations (Table 1). Thus, this segmentation procedure resulted in a distinct set of disturbance metrics for each of the nine annual time series (in Fig. 2 examples of the TCW segmentation). We selected the following metrics describing the segment with the highest magnitude (in the direction of forest loss): (1) the index value for the year before the beginning of the disturbance (hereafter: *prevalue*), (2) the delta of the values of the index between the beginning and end of the disturbance (*magnitude*) and (3) the segment duration (*duration*). We did not apply a threshold filter for the disturbance magnitude (e.g., to disregard low magnitude disturbances). As such, the disturbance metrics included gradual as well as abrupt disturbances (and noise) at this step in our analyses.

3.3. Disturbance mapping

In our third step, we used our LandTrendr disturbance metrics as input for our forest disturbance classification. To generate the training/validation dataset, we used a stratified sampling design where we first trained an initial random forests classifier with an opportunistically collected training sample and then we used the disturbance magnitude class of this initial classification as strata for our sampling. We did this to ensure that our training/validation dataset contained the full range of disturbance magnitudes and a range of different disturbance severities. We then randomly sampled 80 samples per strata (=800 samples in total). We then used the visualization and data collection tool TimeSync (Cohen et al., 2010) to interpret the temporal trajectories at the sample locations. TimeSync facilitates visual interpretation of temporal dynamics in time series, allowing the simultaneous visualization of: (a) Landsat images chips of an area of interest around the target pixel, (b) spectral properties of the pixel time series plotted as a trajectory across time, and (c) very-high-resolution imagery available in Google Earth. A total of 781 samples were successfully interpreted, where 377 samples represented disturbances at any point in time and 404 samples represented undisturbed areas (19 samples were discarded as they were inconclusive). We then combined our training data together with the LandTrendr disturbance metrics (i.e., prevalue, magnitude, and duration) in a random forests classification scheme (Breiman, 2001). We refer to this procedure as secondary classification (Cohen et al., 2018; Wang et al., 2019). All classifications were based on the outputs of 500 decision trees.

Table 1
Values used for LandTrendr parametrization on Google Earth Engine.

Parameter	Value
maxSegments	6
spikeThreshold	0.9
vertexCountOvershoot	3
preventOneYearRecovery	true
recoveryThreshold	0.25
pvalThreshold	0.05
bestModelProportion	0.75
minObservationsNeeded	6

To evaluate how the choice of the seasonal window and vegetation index influenced detection accuracy, we build separate random forests classification models for each of the nine index-season combinations, as well as one ensemble model based on all nine predictor sets (3 disturbance metrics × 9 combinations = 27 variables). We evaluated the classification performance for all 10 classification models following the good practices for accuracy assessment suggested by Olofsson et al. (2014). We used the out-of-bag (OOB) random forests prediction to generate confusion matrices and estimate the overall accuracy and the omission and commission errors. Because random forests takes a bootstrap sample for every tree, the out-of-bag samples can be used for an unbiased estimate of accuracy (Breiman, 2001) In remote sensing studies, resampling techniques are increasingly used to estimate map accuracy, whereas accuracies estimated from single hold-out test datasets are likely to suffer from large variances (Lyons et al., 2018). Finally, we used the best-performing model to generate our final, binary disturbance map (disturbed vs. undisturbed forest).

3.4. Estimating the area of annually disturbed forest

Our ensemble approach provides a consensus map of disturbance happening at any point in our time period, but does not directly yield information on the year of disturbance. To assign a disturbance year to the ensemble map, we used the disturbance year from the LandTrendr segmentation of the best-performing individual disturbance model (i.e., the best performing spectral index and seasonal window). Since we were interested in forest disturbance, but not the permanent conversion from forest to agriculture, we masked converted areas from our analysis using the map by Baumann et al. (2017). Therefore, for all subsequent analyses, our map did not include converted areas (i.e. areas cleared and followed by agricultural land use), but only forest disturbances happening inside forests, thus forest changes that did not result in a change of the land use. We hence attributed the year of disturbance from the best single model to all disturbed pixels of the map resulting from the ensemble classification. We did this only for disturbances occurring after 1989, as disturbance detection in the first two years of time series is typically unreliable (Cohen et al., 2017).

To estimate the area that was disturbed in each year between 1990 and 2017, we again followed best-practice guidelines (Olofsson et al., 2014) and estimated the area based on an independent set of reference locations. We collected a second stratified random sample because the size of our first reference sample was not sufficiently large to estimate disturbed area annually, using the disturbance years in the final (best) disturbance map as strata, using 30 points per strata (=a total of 840 samples as there were 28 years in our times series where disturbance can occur). Each sample was interpreted with TimeSync, labelling the year of disturbance. We then used an unbiased stratified estimator to adjust for possible sampling bias and calculated unbiased area estimates and associated confidence intervals for each year between 1990 and 2017 (Olofsson et al., 2014; Stehman, 2013).

3.5. Comparison with environmental variables

To further assess disturbance patterns, we investigated the relationship between rainfall and soils on the one hand, and disturbances on the other. To assess the relationship of rainfall and disturbance over time, we used the Climate Hazards Group InfraRed Precipitation with Stations data (CHIRPS) time series, which blends infrared geostationary satellite observations with in situ station observations to produce monthly grids of precipitation (Funk et al., 2014). We calculated total annual precipitation, averaged across the study region, and compared this time series with our time series of disturbed forest area. We fitted a linear regression, using total disturbed area as response and average annual precipitation as explanatory variable, and derived residuals.

To explore this relationship further in space, we used the

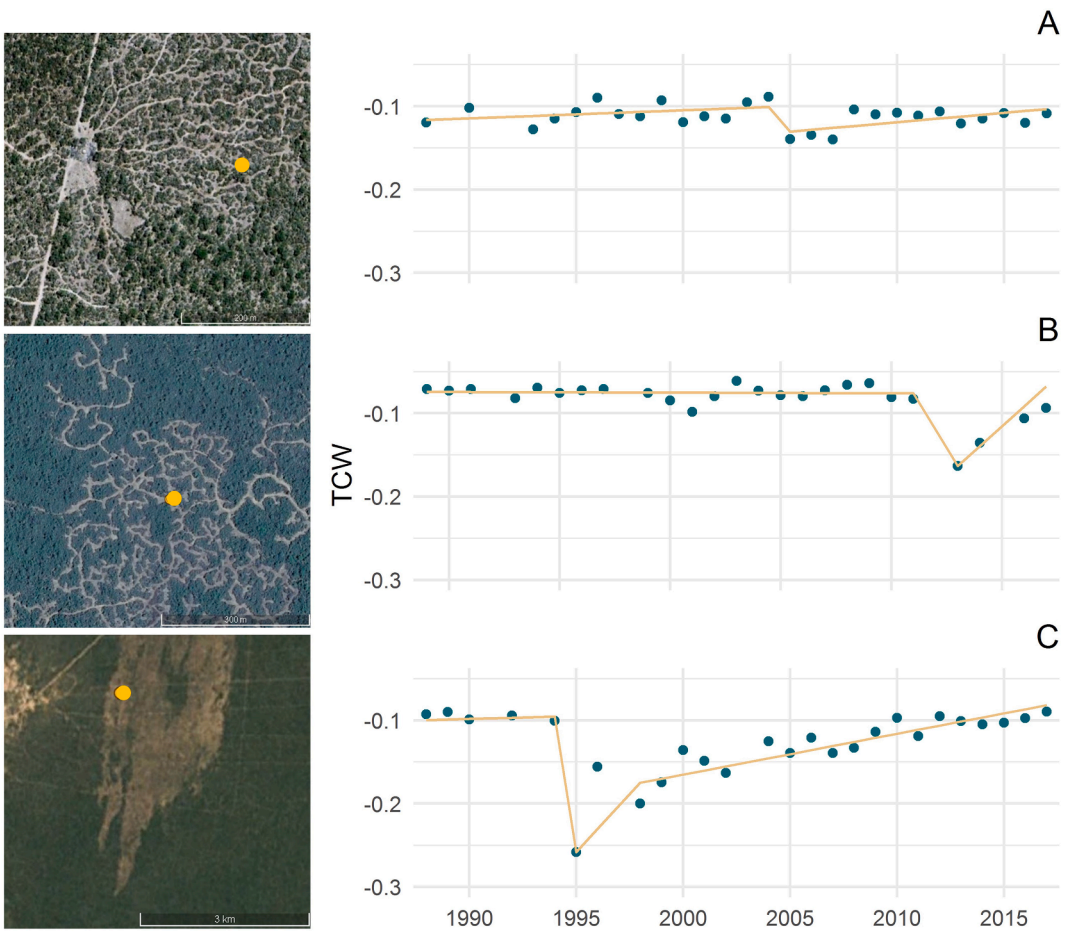

Fig. 2. Three examples of land-use practices leading to forest disturbances, as seen in very-high-resolution satellite images in Google Earth (left), as well as in time series of Tasselled Cap Wetness (TCW) medoids calculated over May-July (right; original annual values in green, values fitted with LandTrendr in yellow). (A) logging for charcoal production (note that the charcoal kiln is also visible); (B) selective logging of valuable tree species; (C) fire. (For interpretation of the references to colour in this figure legend, the reader is referred to the web version of this article.)

Standardized Precipitation Index (SPI) (Mckee et al., 1993) derived from CHIRPS data and compared it with our map of disturbances. SPI values are expressed in standard deviations by which the observed anomaly deviates from the long-term mean. Positive SPI values indicate wet conditions and negative values indicate dry conditions. SPI time series based on CHIRPS data were found to accurately reproduce the occurrence and spatial patterns of wet and dry conditions in Central-Western Argentina (Rivera et al., 2019) and in southern South America (Penalba and Rivera, 2015). We created SPI maps using the Climate Engine tool (Huntington et al., 2017) using a 10-month time-scale (covering the 9 months for which we calculated our spectral-temporal metrics, plus one month before). In addition, we also compared total disturbances with general (average) rainfall patterns by summarizing disturbance for 100-mm-rainfall classes, ranging from 200 mm to 1300 mm. Finally, we summarized disturbances for soil classes using a soil map from the Argentine *Instituto Nacional de Tecnología Agropecuaria* (INTA).

Table 2
Overall accuracy, omission and commission errors of the disturbance detection. The detection of disturbances was based on random forests classifications of LandTrendr-based disturbance metrics, derived for nine combinations of three spectral indices (Tasseled Cap Wetness, Normalized Burn Ratio and Normalized Difference Moisture Index) and three time intervals, as well as an ensemble model over all these variables.

Index/season model	Overall accuracy (%)	Class errors (%)			
		Disturbed		Undisturbed	
		Commission	Omission	Commission	Omission
TCW_Feb_Apr	73.0	35.2	33.0	21.5	23.2
TCW_May_Jul	75.4	31.9	30.5	19.7	20.8
TCW_Aug_Oct	72.6	35.3	34.7	22.3	22.7
NBR_Feb_Apr	69.0	39.2	42.4	26.1	23.7
NBR_May_Jul	71.8	35.2	39.5	24.2	20.9
NBR_Aug_Oct	71.2	36.1	39.9	24.5	21.6
NDMI_Feb_Apr	65.7	43.4	48.4	29.2	25.2
NDMI_May_Jul	69.4	37.8	45.2	26.8	21.2
NDMI_Aug_Oct	66.4	42.4	47.8	27.9	24.6
Ensemble model	78.7	27.3	27.4	17.5	17.4

4. Results

All nine models that we tested for detecting forest disturbances, based on three disturbance metrics derived for one of the combinations of vegetation indices (NDMI, TCW, NBR) and temporal windows (fall, winter, spring), yielded moderate to high detection accuracies. Overall accuracies for individual indices and seasons ranged from 65.7% (NDMI, Feb-Apr) to 75.4% (TCW, May-Jul), with an average accuracy of 71.3% (Table 2). Model performance was generally highest for TCW-based models and lowest for NDMI-based models. There was also a clear pattern in terms of seasons, with composites derived for May-July generally resulting in higher accuracies than composites from other time periods, regardless of the specific index. Validating these models showed that our disturbance detection generally yielded balanced error distributions, with commission errors ranging between 31.9% (TCW, May-Jul) and 43.4% (NDMI, Feb-Apr), and omission errors ranging between 30.5% (TCW, May-Jul) and 48.4% (NDMI, Feb-Apr). Uncertainty was lower for the undisturbed class, with commission errors ranging between 19.7% (TCW, May-Jul) and 29.2% (NDMI, Feb-Apr), and omission errors ranging between 20.8% (TCW, May-Jul) and 25.2% (NDMI, Feb-Apr).

Combining all indices in an ensemble model outperformed any single-index model. The ensemble classification model, using all 27 variables (3 indices × 3 seasons × 3 disturbance metrics), had the highest overall accuracy (79%) as well as the lowest commission error (27.3% for the disturbed class, 17.5% for the undisturbed class) and omission error (27.4% for the disturbed class, 17.4% for the undisturbed class) compared to the models based on disturbance metrics from a single index and season classifications. Furthermore, the ensemble model also had the most balanced distribution of commission and omission errors, which were almost equal within both the disturbed class (around 27%) and the undisturbed class (around 17%). We also explored if LandTrendr results among individual metrics varied more for samples incorrectly classified versus those correctly classified, but found no difference (results not shown).

The final disturbance map, showing disturbed vs. undisturbed areas, highlighted distinct spatial patterns across the Argentine Dry Chaco (Fig. 3). Disturbances between 1990 and 2017 were generally more widespread at the interfaces of larger forested and non-forested patches (e.g., in the southernmost section of the study area corresponding to the province of San Luis), inside fragmented forest patches (e.g., in the south-western part of Chaco province, eastern side of Santiago del Estero province, north-eastern part of Córdoba province), as well as close to water bodies such as major rivers (e.g., the Pilcomayo river in the north of Formosa, or along the Río Dulce in Santiago del Estero). In contrast, large, continuous patches of remaining forest appear less affected by disturbance, particularly in the southwest of the study region (provinces of San Luis, San Juan and western La Rioja) and in the north-western Chaco province. Provinces of Córdoba, Santiago del Estero and Catamarca showed the highest disturbance rates (respectively 13%, 12% and 11%). Examining the disturbance map also show distinct and diverse spatial patterns of detected disturbances from larger, continuous patches (e.g., Fig. 3A) to more dispersed and irregular patterns (e.g., Fig. 3B), pointing to diverse disturbance agents.

Taking a closer look at the timing of disturbance, based on the best-performing model for any combination of spectral index and season (i.e., TCW, May-July) provided further insights into the spatiotemporal patterns of forest disturbance across the Argentine Chaco (Fig. 3). Larger disturbance patches occurred predominately in the beginning of our observation period, in the 1990 s, with several large, irregularly shaped patches (e.g., at the border between La Rioja and Córdoba provinces and in central Santiago del Estero). More recently, disturbances patches became generally smaller and had more geometrical shapes (indicated in our map by warmer colours, Fig. 3). Such disturbances occurred

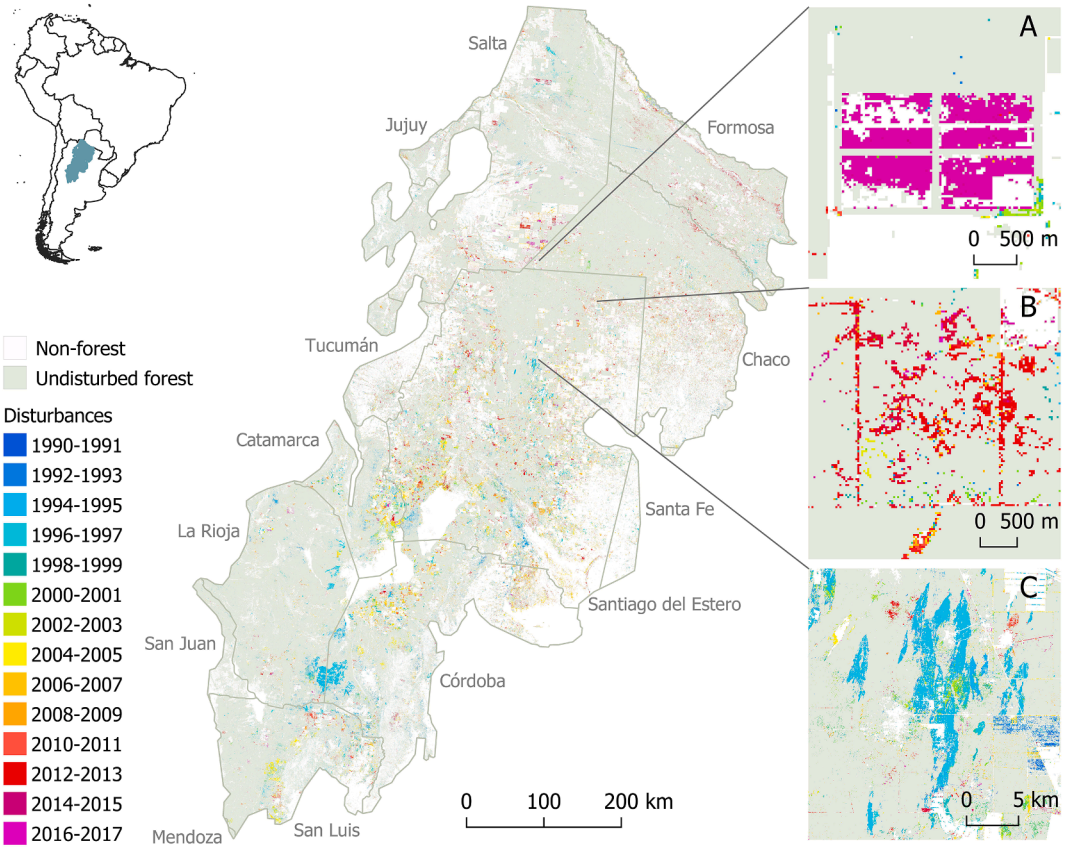

Fig. 3. Year of detection of disturbances map produced by merging the disturbance map from the ensemble model and the best single index model (TCW, May-July).

mainly close to existing agricultural fields, for example at the southern border between Salta and Chaco provinces and in the north-western part of Cordoba and south-western Catamarca. In addition, clear overall spatiotemporal patterns were visible with disturbances more prevalent in the south in the early 1990s, but progressively moving towards the more interior Chaco over time.

The estimated annual area of forest disturbances, based on an independent set of ground truth points not used in model training, showed a variable pattern over time (Fig. 4, B). On average, about 888 km^2 (standard deviation = 581 km^2) of the remaining forest in 2018 was disturbed over time, yet this varied in magnitude from year to year. Highest disturbed areas occurred in 1995, 2004, 2009 and 2013 with more than 1500 km^2 of disturbed areas, with a remarkable peak in 2013 when 2647 km^2 were disturbed (95% confidence interval = ±488 km^2). Conversely, we found very small areas of disturbance for the years 1990 to 1993, 1998, 2002 and 2014 to 2016 (all < 500 km^2), with the lowest area estimated for 1990 (48 ± 42 km^2). The total area of disturbed forest across our entire study period was 24,877 ± 860 km^2.

Comparing the temporal patterns of disturbed area with precipitation time series revealed synced patterns (Fig. 4) between estimated annual disturbed area (panel B) and cumulative annual precipitation (panel A). In particular, peaks in the disturbance time series typically corresponded to years with particularly low precipitation (e.g., in 1995 and 2013). Conversely, the three years with highest rainfall (1991, 2002, and 2015) had very low levels of disturbed areas (all below 400 km^2). However, plotting the residuals of a simple linear regression model (Fig. 5) between annual disturbed area and annual precipitation suggested that the effect of precipitation on forest disturbances was not consistent over time (Fig. 4, panel C). The coefficient of determination also corroborates that precipitation alone does not explain disturbed area (R^2 = 0.41).

Comparing the spatial disturbances patterns with maps of drought index (SPI; Fig. 6) provided further insights into the relationship between precipitation and disturbances. The drought index revealed a remarkably high spatial variability, with hotspots occurring in distinct regions of the Argentine Dry Chaco (e.g., 1995, 2004 and 2013, when

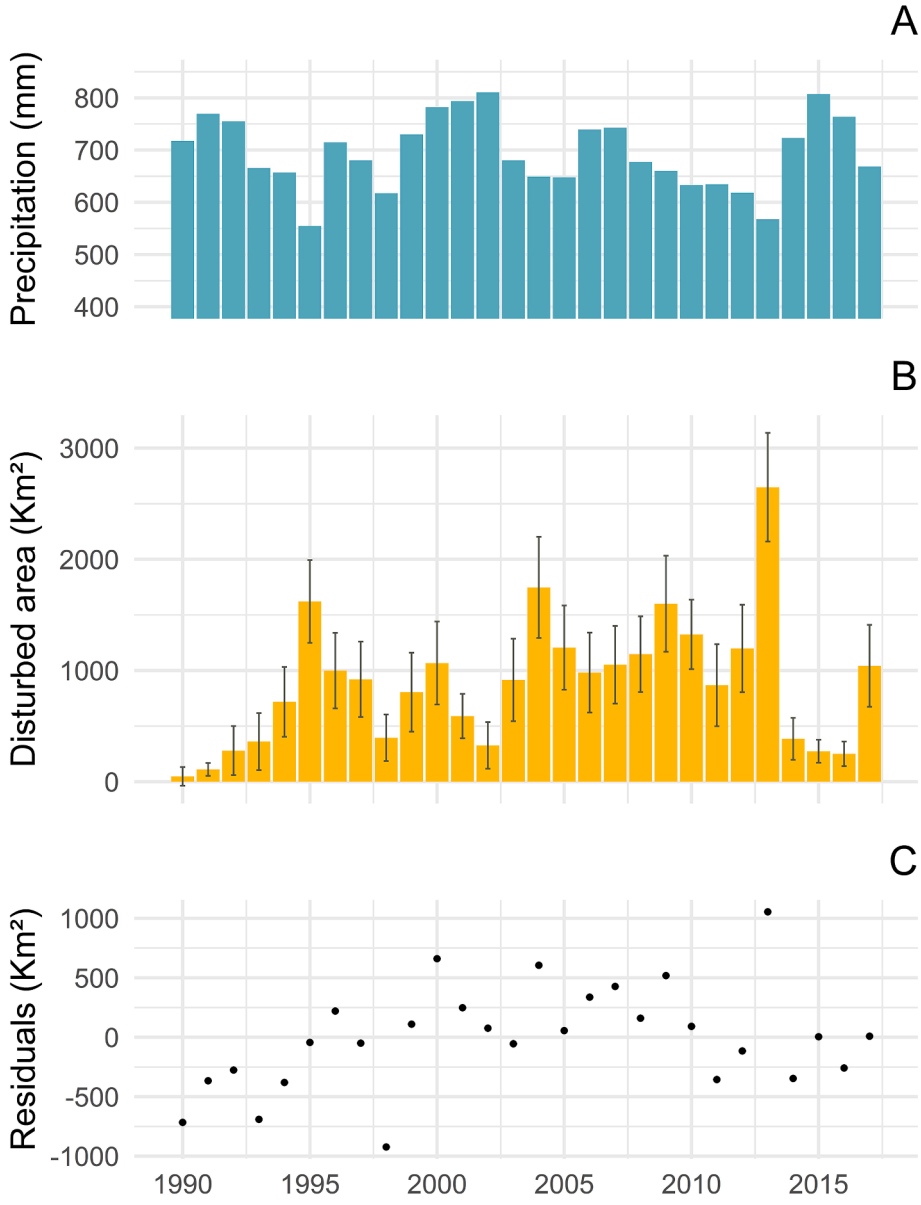

Fig. 4. Comparison between disturbances and annual precipitation patterns. (A) annual precipitation sums derived from CHIRPS data. (B) annual disturbance area estimated from Landsat composites. (C): residuals between the observed (Landsat) and predicted disturbed area (predicted based on a linear regression between observed area and precipitations, see Fig. 5).

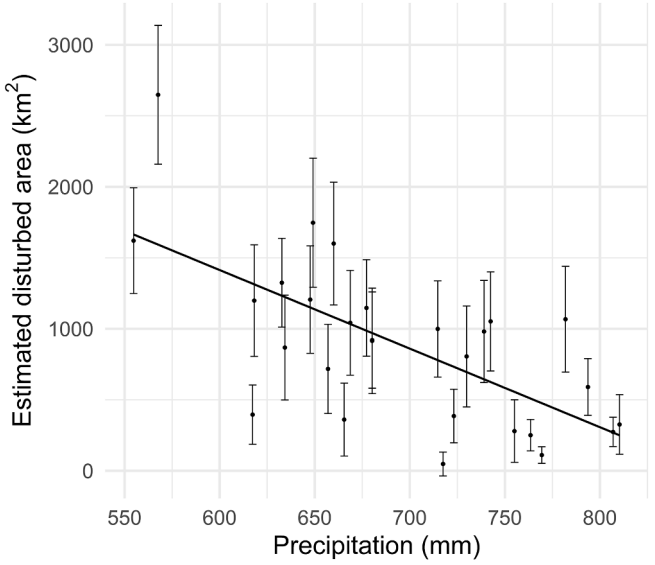

Fig. 5. Linear regression model fitted to annual precipitation sums derived from CHIRPS data and annual disturbance area estimated from Landsat composites.

rainfall was lowest). For instance, drought hotspots in 1995 occurred in the central and southern part of the study area, whereas the northern part of the study region was hit hardest in 2013. Interestingly, some of these spatial patterns were also reflected in the disturbance maps (Fig. 6, lower row), with regions with relatively high disturbance densities occurring where drought impacts were particularly high in a given year. Yet, disturbances also occur in areas not affected by drought.

Finally, summarizing disturbances along a gradient of average rainfall over the entire observation period (1990–2017) showed clear association of disturbance with average rainfall in our study region (Fig. 7). In absolute terms, disturbed areas followed a clearly hump-shaped distribution, with largest forest disturbance areas found at average rainfall around 700 mm (Fig. 7A), where also forest cover in the Dry Chaco is still the highest. Putting the disturbed area in relation to the remaining forest extent in these rainfall zones showed that highest disturbance rates occurred above 500 mm (constantly above 8–10% across the entire observation period). At lower average rainfall, disturbance rates were much lower (<4%). In terms of soil types, disturbed areas were highest in Mollisols (Fig. 7 C), with Alfisols and Mollisols having the highest disturbance rates (around 9%). Generally, disturbance rates varied less in relation to soil types than in relation to average precipitation patterns.

5. Discussion

Tropical dry forests experience high human pressure, but monitoring forest degradation in these systems is challenging due to high canopy complexity, strong phenology, high climate variability, and diverse degradation drivers. Making full use of the opportunities that the Landsat archive provides, we here provide an assessment of forest degradation in the Dry Chaco, a large tropical dry forest region (489,000 km^2), over a 30-year time span using dense Landsat time series, temporal segmentation, and an ensemble disturbance detection algorithm. Methodologically, our study showed that forest disturbances associated with forest degradation can be mapped reliably and that a multispectral ensemble approach is preferable to time-series analyses based on individual spectral indices. Thematically, our study yielded three main insights. First, we found major areas (about 25,000 km2, 8% of the forested area) of the remaining forests in the Argentine Dry Chaco have been disturbed since 1990, suggesting degradation is a widespread phenomenon that deserves more attention in discussions of environmental sustainability in the Chaco. Second, we found diverse spatial patterns of forest disturbances, which appear to be driven by different disturbance agents, including both natural (e.g., drought) and anthropogenic ones (e.g., logging, agricultural fires). This suggests disturbance attribution is central for understanding the drivers and impacts of forest degradation. Third, we found a clear association between forest disturbance and precipitation. Temporally, forest disturbance was particularly widespread during drought years. Our disturbance maps suggest a possible link of drought and increased fire activities can explain this pattern. Spatially, forest disturbance was most widespread in areas with average rainfall around 700 mm (Fig. 6A). These are areas that are too dry for cropping, and therefore still contain considerable shares of forest, yet are inhabited by more people than the even drier parts of the Chaco. Together, this can explain the hump-shaped disturbance distribution we find. More generally, our analyses suggest that an improved degradation monitoring is urgently needed in the world's tropical dry forests. Our approach based on the Landsat archives and trajectory analyses, both readily implemented in Google Earth Engine, are promising for scaling up monitoring efforts.

Our study demonstrates the feasibility of mapping disturbances robustly across a large tropical and subtropical dry forest. Our overall accuracy (about 79%) is comparable to the only other study adopting a similar approach for a tropical dry forest (Wang et al. (2019). In this study a spectral ensemble was used to map disturbances in different forest types in Mato Grosso, yielding an overall accuracy of about 83% for the tropical dry forest area assessed (a much smaller area than in our study). Likewise, our overall accuracies are comparable to those obtained in moist tropical forests, such as in Brazil, Ethiopia and Vietnam (Schultz et al., 2016). All of this further attests to the robustness of our approach. However, it should be noted that the Chaco is relatively homogeneous in terms of topography (Bucher, 1982) and transferring our approach to topographically more complex woodlands, such as in Central America or Colombia, might therefore bring new challenges due to complexity arising from illumination differences.

Our study adds to growing evidence that a multispectral ensemble approach outperforms traditional algorithms for disturbance detection. The ensemble performed better than any single index with improved classification accuracy and error balance, a finding consistent with studies by Cohen et al. (2018), Schultz et al. (2016) and Wang et al. (2019). In terms of the performance of single indices, our study suggests that particularly the Tasseled Cap Wetness component has considerable potential for advancing degradation monitoring in tropical dry forests. This index outperformed all other indices in our change detection model comparison, in line with prior work on different forest types (Cohen et al., 2018; Czerwinski et al., 2014; DeVries et al., 2016). For tropical dry forests, Grogan et al. (2015) found TCW to be best-performing for monitoring forest disturbances, while other studies found NDMI (the least-performing index in our case) or NBR to be useful for detecting disturbances (Schneibel et al., 2017; Smith et al., 2019). This diversity of findings, not always from studies that compared across multiple indices, further highlights a strength of an ensemble approach, which does not force an *a priori* selection of a specific spectral metric. Given the diversity of disturbance signatures we found in our case, using multiple spectral indices in an ensemble approach might also provide opportunities to capture this diversity (as different indices might detect different disturbances best), though quantifying this requires further work.

Our assessment of disturbed areas indicates that a large share, about 8% (=24,877 ± 860 km^2) of the forests spared so far from agricultural conversion were affected by forest disturbances in the period 1990–2017. This area represents roughly one third of the area that was converted to agriculture during that time. For instance, forest conversion to agriculture in our study area in the period 1985 to 2013 amounted to 74,351 km^2 (Baumann et al., 2017). These forest losses are associated with globally-relevant carbon emissions (Baldassini et al., 2020; Baumann et al., 2017; Gasparri et al., 2008) and biodiversity loss (Romero-Muñoz et al., 2020, 2019; Semper-Pascual et al., 2020, 2018).

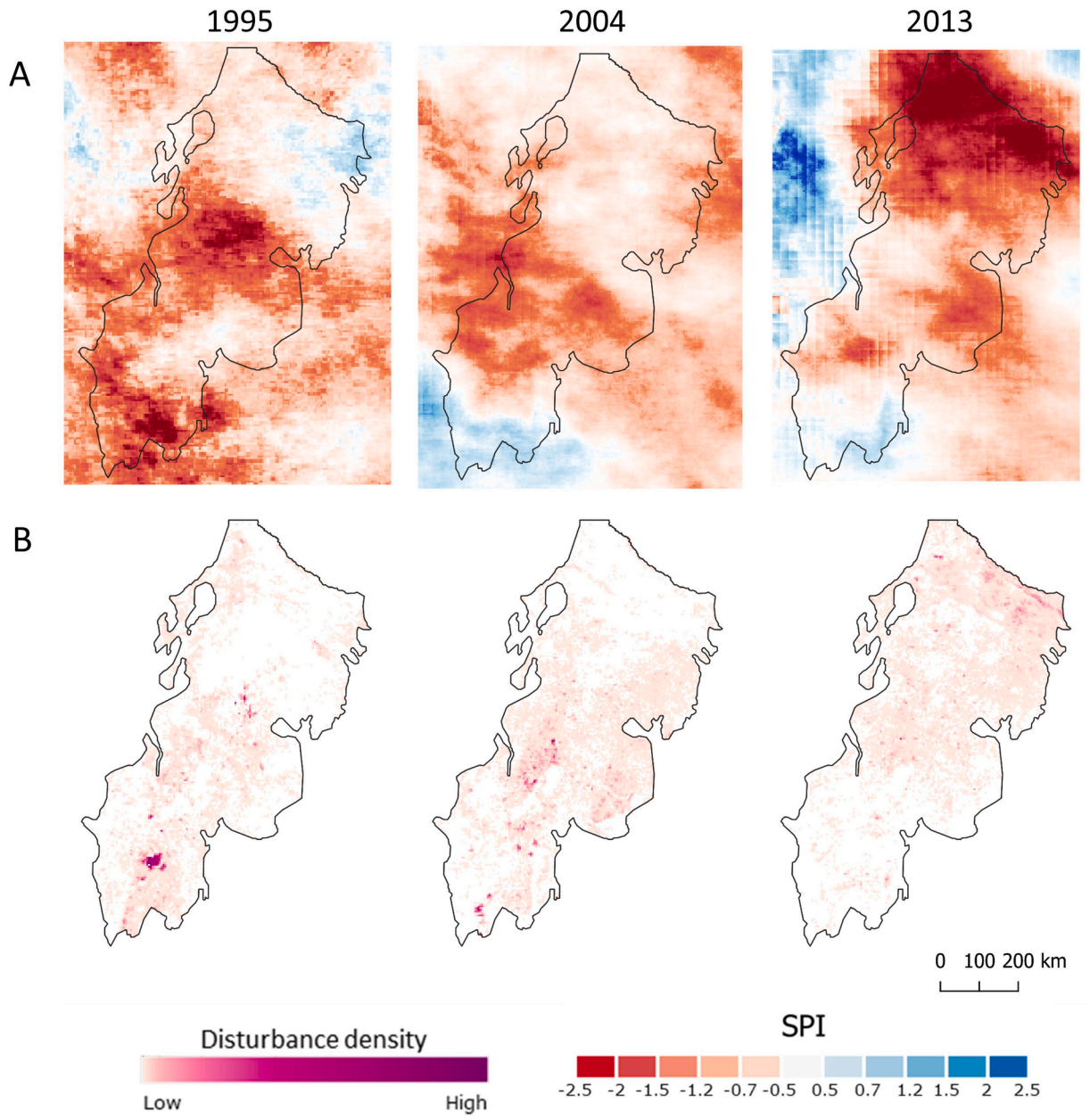

Fig. 6. Spatial comparison between drought impact and disturbance patterns for the years 1995 (left), 2004 (centre), and 2013 (right). (A) Standardized Precipitation Index maps based on CHIRPS data; (B) disturbance density maps. These three years had particularly low rainfall and large disturbed areas.

Yet all impact assessments so far have exclusively focussed on full forest conversion, as ours is to the best of our knowledge the first study quantifying the extent of forest disturbance within remaining forests. As a result, a key finding of our work is that, unfortunately, the strong environmental impacts of forest loss and transformation reported for the Chaco (Barral et al., 2020; Baumann et al., 2017; Piquer-Rodríguez et al., 2015) still represent a substantial underestimation of the real impacts, and simple forest vs non-forest maps might heavily overestimate the quality of the remaining Chaco forests. Impact assessments must therefore urgently include forest-degradation indicators, such as the extent and severity of disturbances that we derive here. This seems particularly relevant for assessments of Reducing Emissions from Deforestation and forest Degradation (REDD+) implementation, particularly when setting baselines against which to measure reduction in forest conversion and degradation. These baselines do so far not consider degradation footprints and extent (SAyDS, 2019), which is to a large extent due to missing disturbance maps prior to our study.

Although we did not attempt here to differentiate between disturbance agents, both the shape and context of disturbance patterns hint to the processes causing disturbances. For example, irregular, continuous patches might be attributable to fires (e.g., Fig. 3C). Such patches often occurred next to agricultural fields, suggesting that post-harvest burns and fires escaping to nearby forests are a major driver of forest disturbance in the Chaco. In contrast, we found many large, rectangular patches of disturbed forest (e.g., Fig. 3A) – typically in areas where the agricultural frontiers are advancing (le Polain de Waroux et al., 2018). This can be interpreted as evidence for forest clearing with the intention to establish agriculture, but this intention was never realized. As a result, forests were only cleared partially and/or cleared areas were abandoned with subsequent woodland recovery, a pattern so far not documented for the Chaco. In addition to these larger disturbance patches, we found many small disturbances (e.g., Fig. 3B) which appear to be related to selective logging or charcoal production (Rueda et al., 2015). Finally, linear disturbances were frequent, likely due to the construction or

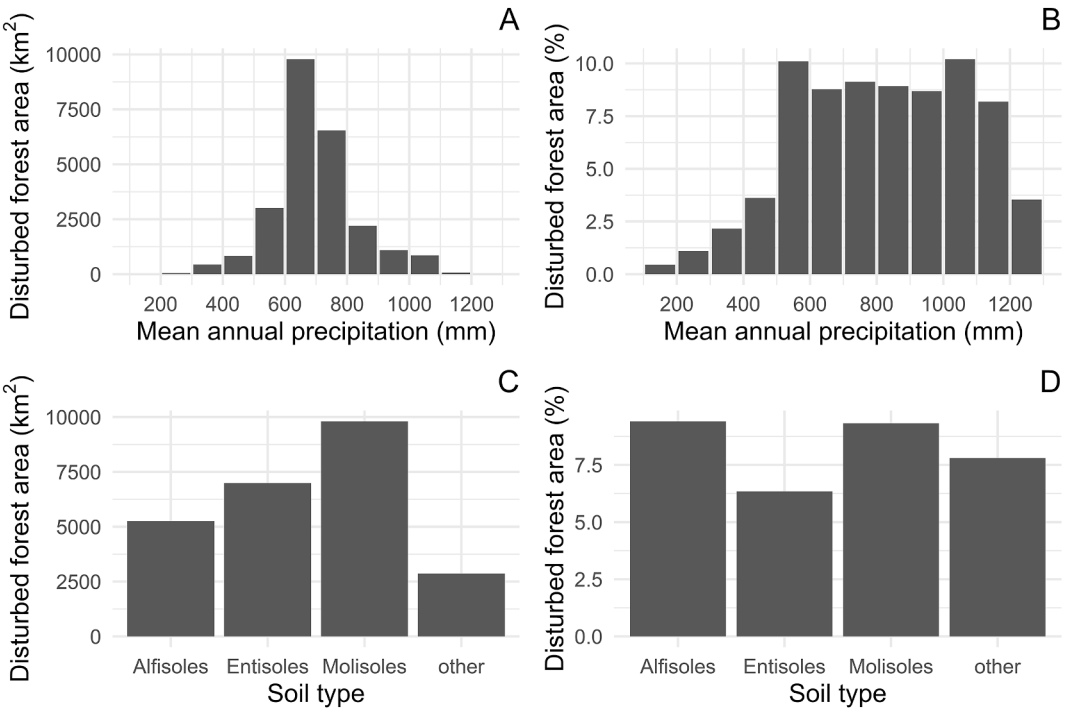

Fig. 7. Forest disturbances between 1990 and 2017 in the Argentine Dry Chaco in relation to average annual precipitation rainfall gradient and soil types. (A) Total disturbed area (24,877 km^2) by average precipitation zone; (B) Percentage of forest disturbed over total forest area by average precipitation zone; (C) Total disturbed area by soil type; (D) Percentage of forest disturbed by soil type.

maintenance of forest roads. In sum, the spatial features of disturbance suggest diverse disturbance agents, and combining our data with ancillary data on these agents would be a beneficial follow-up step that can provide insights into the underlying causes and possible policy responses of forest degradation (Finer et al., 2018).

A key finding of our work was a possible link between the forest disturbance and drought years, with the largest area of disturbance corresponded to the most extreme droughts in our study area (Fig. 5). Similar patterns were found in the Amazon, possibly due to drought-related fires (Bullock et al., 2020). This link has been suggested for the Chaco too (Argañaraz et al., 2015; Fischer et al., 2012), and is further corroborated by our work as we found fire-like disturbance patterns particularly in drought years and particularly in areas highlighted in the SPI maps as drought hotspots (Fig. 5). We speculate that fires are more likely to occur and escape (e.g., when fields are burned), and likely larger, during drought years. However, droughts impact forest also directly (Corlett, 2016) and our analyses suggest that particularly forests along rivers are susceptible to drought impacts, possibly because these forest are more dependent on water resources and vulnerable to water stress.

Focussing on the link between disturbance and average rainfall across the Chaco, our results suggest the majority of disturbances occurred around 700 mm annual precipitation. This is perhaps not surprising, as this precipitation amount represents the lower limit for major crops (e.g. soybean, maize) in the Chaco (Grau et al., 2005), and thus deforestation occurs mainly in areas with higher precipitation (Zak et al., 2008). Several processes suggest this could be changing in the future. First, the silvopastoral cattle ranching systems mentioned above are economically feasible at precipitation levels below 700 mm and we already find evidence for their expansion (Peri et al., 2017). Second, new soybean strains that can tolerate drier climates are being developed, and this would likely shift the deforestation frontiers in major ways (Leguizamón, 2014). That the bulk of the forest disturbances in the remaining forest occurred in relatively wet areas (i.e. between 500 mm and 1200 mm) can likely be explained by the higher presence of people (both farmers and forest smallholders) in these, relatively-speaking, more favourable areas compared to the driest parts of the Chaco. Also, this pattern might be explained by the lower availability or quality of forest resources in extremely dry areas, where some valuable species disappear and vegetation grows slower and less high (Powell et al., 2018; Prado, 1993).

While our methodology resulted in relatively high detection probability and an overall robust forest disturbances map across a large region, three limitations need to be mentioned. First, our classification was based on training and validation data that were visually interpreted from Landsat image trajectories and very high-resolution images on Google Earth. Subtle disturbances (e.g., selective logging) are not easy to identify in such a way and might be missed. This suggests our estimate of forest disturbance is likely conservative. Second, and related to this, our disturbance map does not capture the impact of forest grazing on forest understory, which is a key driver of forest degradation in the Chaco (Adamoli et al., 1990; Bucher and Huszar, 1999; Torrella and Adámoli, 2005). Combining our approach with approaches that use radar or lidar data (Dubayah et al., 2020) may help to monitor such more subtle disturbances in the future. It is also worth mentioning that by considering only disturbances and not recovery, our map gives a partial picture of forest dynamics. Taking into account regrowth would be important for carbon budget estimates. However, both in the context of forest degradation and for carbon accounting, assessing recovery would require separating trees and shrubs, as the latter often dominates in recovering forests that had contained tall trees before they were disturbed. Our segments are based on spectral recovery only and do therfore not readily separate shrub from tree cover. Interpreting them as forest recovery could therefore hide ongoing degradation, which is why we refrain from showing them here. Lastly, we cannot rule out a systematic bias in the finding of higher disturbances found in dry years. Detection, however, could be both positively biased (e.g., better detectability due to lower cloud cover) or negatively biased (e.g., less contrast between vegetation and background). Generally, we are convinced our estimates in dry years are reliable, because cloud cover is lowest and image availability very good for dry seasons across our observation period.

In this study, we demonstrated the benefit of a Landsat-based,

spectral ensemble approach to map forest disturbances in tropical dry forests. Most elements of our approach are implemented in Google Earth Engine, providing considerable potential for upscaling and thus for degradation-related forest disturbance monitoring. Our study highlights that such monitoring is important and timely, given the rapid pace at which tropical dry forests around the globe are disappearing, and the so far overlooked extent of disturbances related to degradation in our case. The Gran Chaco is a global hotspot of deforestation (Hansen et al., 2013), and our work suggests this is still an underestimation of the real impact of land use on forest loss and transformation. Stepping up forest disturbance monitoring in tropical dry forests is urgently needed to better understand carbon emissions and biodiversity loss associated with forest loss – and to identify effective strategies to mitigate these losses.

CRediT authorship contribution statement

Teresa De Marzo: Conceptualization, Data curation, Formal analysis, Methodology, Writing - original draft. **Dirk Pflugmacher:** Methodology, Writing - review & editing. **Matthias Baumann:** Methodology, Writing - review & editing. **Eric F. Lambin:** Conceptualization, Funding acquisition, Writing - review & editing. **Ignacio Gasparri:** Conceptualization, Writing - review & editing. **Tobias Kuemmerle:** Conceptualization, Funding acquisition, Supervision, Writing - review & editing.

Declaration of Competing Interest

The authors declare that they have no known competing financial interests or personal relationships that could have appeared to influence the work reported in this paper.

Acknowledgements

This research was funded by the Belgian Federal Science Policy Office Research Programme for Earth Observation (belspo-STEREO-III, project REFORCHA, SR/00/338), by the Federal Ministry of Education and Science (BMBF, 460 project PASANOA, 031B0034A), and the German Research Foundation (DFG, project KU 2458/5-1).

References

Adamoli, J., Sennhauser, E., Acero, J.M., Rescia, A., 1990. Stress and disturbance: vegetation dynamics in the dry Chaco region of Argentina. J. Biogeogr. 17, 147–156.

Argañaraz, J.P., Pizarro, G.G., Zak, M., Bellis, L.M., 2015. Fire regime, climate, and vegetation in the Sierras de Córdoba. Argentina. Fire Ecol. 11, 55–73. https://doi.org/10.4996/fireecology.1101055.

Asner, G.P., Knapp, D.E., Broadbent, E.N., Oliveira, P.J.C., Keller, M., Silva, J.N., 2005. Selective Logging in the Brazilian Amazon. Science 310, 480–482. https://doi.org/10.1126/science.1118051.

Bachmann, L., Daniele, C., Mereb, J., Frassetto, A., 2007. Identificación expeditiva de los principales problemas ambientales en el Gran Chaco argentino. Instituto de Geografía - UBA.

Baldassini, P., Bagnato, C.E., Paruelo, J.M., 2020. How may deforestation rates and political instruments affect land use patterns and Carbon emissions in the semi-arid Chaco, Argentina? Land Use Policy 99, 104985. https://doi.org/10.1016/j.landusepol.2020.104985.

Barral, M.P., Villarino, S., Levers, C., Baumann, M., Kuemmerle, T., Mastrangelo, M., 2020. Widespread and major losses in multiple ecosystem services as a result of agricultural expansion in the Argentine Chaco. J. Appl. Ecol. 1–14. https://doi.org/10.1111/1365-2664.13740.

Baumann, M., Gasparri, I., Piquer-Rodríguez, M., Gavier Pizarro, G., Griffiths, P., Hostert, P., Kuemmerle, T., 2017. Carbon emissions from agricultural expansion and intensification in the Chaco. Glob. Chang. Biol. 23, 1902–1916. https://doi.org/10.1111/gcb.13521.

Betts, M.G., Wolf, C., Ripple, W.J., Phalan, B., Millers, K.A., Duarte, A., Butchart, S.H.M., Levi, T., 2017. Global forest loss disproportionately erodes biodiversity in intact landscapes. Nature 547, 441–444. https://doi.org/10.1038/nature23285.

Breiman, L., 2001. Random forests. Mach. Learn. 45, 5–32. https://doi.org/10.1023/A:1010933404324.

Bucher, E.H., 1982. Chaco and Caatinga — South American Arid Savannas, Woodlands and Thickets, pp. 48–79. doi:10.1007/978-3-642-68786-0_4.

Bucher, E.H., Huszar, P.C., 1999. Sustainable management of the Gran Chaco of South America: Ecological promise and economic constraints. J. Environ. Manage. 57, 99–108. https://doi.org/10.1006/jema.1999.0290.

Bullock, E.L., Woodcock, C.E., Holden, C.E., 2019. Improved change monitoring using an ensemble of time series algorithms. Remote Sens. Environ., 111165 https://doi.org/10.1016/j.rse.2019.04.018.

Bullock, E.L., Woodcock, C.E., Souza, C., Olofsson, P., 2020. Satellite-based estimates reveal widespread forest degradation in the amazon. Glob. Chang. Biol. gcb.15029 https://doi.org/10.1111/gcb.15029.

Cabido, M., Zeballos, S.R., Zak, M., Carranza, M.L., Giorgis, M.A., Cantero, J.J., Acosta, A.T.R., 2018. Native woody vegetation in central Argentina: classification of chaco and espinal forests. Appl. Veg. Sci. 1–14. https://doi.org/10.1111/avsc.12369.

Cohen, W.B., Healey, S.P., Yang, Z., Stehman, S.V., Brewer, C.K., Brooks, E.B., Gorelick, N., Huang, C., Hughes, M.J., Kennedy, R.E., Loveland, T.R., Moisen, G.G., Schroeder, T.A., Vogelmann, J.E., Woodcock, C.E., Yang, L., Zhu, Z., 2017. How similar are forest disturbance maps derived from different Landsat time series algorithms? Forests 8, 1–19. https://doi.org/10.3390/f8040098.

Cohen, W.B., Yang, Z., Healey, S.P., Kennedy, R.E., Gorelick, N., 2018. A LandTrendr multispectral ensemble for forest disturbance detection. Remote Sens. Environ. 205, 131–140. https://doi.org/10.1016/j.rse.2017.11.015.

Cohen, W.B., Yang, Z., Kennedy, R., 2010. Detecting trends in forest disturbance and recovery using yearly Landsat time series: 2. TimeSync — Tools for calibration and validation. Remote Sens. Environ. 114, 2911–2924. https://doi.org/10.1016/j.rse.2010.07.010.

Corlett, R.T., 2016. The impacts of droughts in tropical forests. Trends Plant Sci. 21, 584–593. https://doi.org/10.1016/j.tplants.2016.02.003.

Czerwinski, C.J., King, D.J., Mitchell, S.W., 2014. Mapping forest growth and decline in a temperate mixed forest using temporal trend analysis of Landsat imagery, 1987–2010. Remote Sens. Environ. 141, 188–200. https://doi.org/10.1016/j.rse.2013.11.006.

Da Ponte, E., Fleckenstein, M., Leinenkugel, P., Parker, A., Oppelt, N., Kuenzer, C., 2015. Tropical forest cover dynamics for Latin America using Earth observation data: a review covering the continental, regional, and local scale. Int. J. Remote Sens. 36, 3196–3242. https://doi.org/10.1080/01431161.2015.1058539.

DeVries, B., Pratihast, A.K., Verbesselt, J., Kooistra, L., Herold, M., 2016. Characterizing forest change using community-based monitoring data and Landsat time series. PLoS One 11, e0147121. https://doi.org/10.1371/journal.pone.0147121.

Dubayah, R., Blair, J.B., Goetz, S., Fatoyinbo, L., Hansen, M., Healey, S., Hofton, M., Hurtt, G., Kellner, J., Luthcke, S., Armston, J., Tang, H., Duncanson, L., Hancock, S., Jantz, P., Marselis, S., Patterson, P.L., Qi, W., Silva, C., 2020. The global ecosystem dynamics investigation: high-resolution laser ranging of the earth's forests and topography. Sci. Remote Sens. 1, 100002 https://doi.org/10.1016/j.srs.2020.100002.

Fehlenberg, V., Baumann, M., Gasparri, N.I., Piquer-Rodriguez, M., Gavier-Pizarro, G., Kuemmerle, T., 2017. The role of soybean production as an underlying driver of deforestation in the South American Chaco. Glob. Environ. Chang. 45, 24–34. https://doi.org/10.1016/j.gloenvcha.2017.05.001.

Finer, B.M., Novoa, S., Weisse, M.J., Petersen, R., Mascaro, J., Souto, T., Stearns, F., Martinez, R.G., 2018. Combating deforestation: from satellite to intervention. Science 360, 1303–1305. https://doi.org/10.1126/science.aat1203.

Fischer, M.A., Di Bella, C.M., Jobbágy, E.G., 2012. Fire patterns in central semiarid Argentina. J. Arid Environ. 78, 161–168. https://doi.org/10.1016/j.jaridenv.2011.11.009.

Flood, N., 2013. Seasonal Composite Landsat TM/ETM+ Images Using the Medoid (a Multi-Dimensional Median). Remote Sens. 5, 6481–6500. https://doi.org/10.3390/rs5126481.

Foga, S., Scaramuzza, P.L., Guo, S., Zhu, Z., Dilley, R.D., Beckmann, T., Schmidt, G.L., Dwyer, J.L., Joseph Hughes, M., Laue, B., 2017. Cloud detection algorithm comparison and validation for operational Landsat data products. Remote Sens. Environ. 194, 379–390. https://doi.org/10.1016/j.rse.2017.03.026.

Funk, C.C., Peterson, P.J., Landsfeld, M.F., Pedreros, D.H., Verdin, J.P., Rowland, J.D., Romero, B.E., Husak, G.J., Michaelsen, J.C., Verdin, A.P., 2014. A quasi-global precipitation time series for drought monitoring. U.S. Geol. Surv. Data Ser. 832, 4. https://doi.org/10.3133/ds832.

Gao, B.C., 1996. NDWI - A normalized difference water index for remote sensing of vegetation liquid water from space. Remote Sens. Environ. 58, 257–266. https://doi.org/10.1016/S0034-4257(96)00067-3.

Gasparri, N.I., Grau, H.R., 2009. Deforestation and fragmentation of Chaco dry forest in NW Argentina (1972–2007). For. Ecol. Manage. 258, 913–921. https://doi.org/10.1016/j.foreco.2009.02.024.

Gasparri, N.I., Grau, H.R., Manghi, E., 2008. Carbon pools and emissions from deforestation in extra-tropical forests of northern Argentina between 1900 and 2005. Ecosystems 11, 1247–1261. https://doi.org/10.1007/s10021-008-9190-8.

Gibson, L., Lee, T.M., Koh, L.P., Brook, B.W., Gardner, T.A., Barlow, J., Peres, C.A., Bradshaw, C.J.A., Laurance, W.F., Lovejoy, T.E., Sodhi, N.S., 2011. Primary forests are irreplaceable for sustaining tropical biodiversity. Nature 478, 378–381. https://doi.org/10.1038/nature10425.

Goetz, S.J., Hansen, M., Houghton, R.A., Walker, W., Laporte, N., Busch, J., 2015. Measurement and monitoring needs, capabilities and potential for addressing reduced emissions from deforestation and forest degradation under REDD+. Environ. Res. Lett. 10, 123001 https://doi.org/10.1088/1748-9326/10/12/123001.

Grainger, A., 1993. Controlling tropical deforestation, Controlling tropical deforestation. Earthscan Publications Ltd, London. doi:10.2307/3059951.

Grau, H.R., Gasparri, N.I., Aide, T.M., 2008. Balancing food production and nature conservation in the Neotropical dry forests of northern Argentina. Glob. Chang. Biol. 14, 985–997. https://doi.org/10.1111/j.1365-2486.2008.01554.x.

Grau, H.R., Gasparri, N.I., Aide, T.M., 2005. Agriculture expansion and deforestation in seasonally dry forests of north-west Argentina. Environ. Conserv. 32, 140. https://doi.org/10.1017/S0376892905002092.
Grogan, K., Pflugmacher, D., Hostert, P., Kennedy, R., Fensholt, R., 2015. Cross-border forest disturbance and the role of natural rubber in mainland Southeast Asia using annual Landsat time series. Remote Sens. Environ. 169, 438–453. https://doi.org/10.1016/j.rse.2015.03.001.
Hansen, M.C.C., Potapov, P.V., Moore, R., Hancher, M., Turubanova, S.A.A., Tyukavina, A., Thau, D., Stehman, S.V.V., Goetz, S.J.J., Loveland, T.R.R., Kommareddy, A., Egorov, A., Chini, L., Justice, C.O.O., Townshend, J.R.G.R.G., 2013. High-resolution global maps of 21st-century forest cover change. Science 342, 850–853. https://doi.org/10.1126/science.1244693.
Healey, S.P., Cohen, W.B., Yang, Z., Kenneth Brewer, C., Brooks, E.B., Gorelick, N., Hernandez, A.J., Huang, C., Joseph Hughes, M., Kennedy, R.E., Loveland, T.R., Moisen, G.G., Schroeder, T.A., Stehman, S.V., Vogelmann, J.E., Woodcock, C.E., Yang, L., Zhu, Z., 2018. Mapping forest change using stacked generalization: An ensemble approach. Remote Sens. Environ. 204, 717–728. https://doi.org/10.1016/j.rse.2017.09.029.
Hethcoat, M.G., Edwards, D.P., Carreiras, J.M.B., Bryant, R.G., França, F.M., Quegan, S., 2019. A machine learning approach to map tropical selective logging. Remote Sens. Environ. 221, 569–582. https://doi.org/10.1016/j.rse.2018.11.044.
Hirschmugl, M., Steinegger, M., Gallaun, H., Schardt, M., 2014. Mapping forest degradation due to selective logging by means of time series analysis: case studies in Central Africa. Remote Sens. 6, 756–775. https://doi.org/10.3390/rs6010756.
Hislop, S., Jones, S., Soto-Berelov, M., Skidmore, A., Haywood, A., Nguyen, T.H., 2019. A fusion approach to forest disturbance mapping using time series ensemble techniques. Remote Sens. Environ. 221, 188–197. https://doi.org/10.1016/j.rse.2018.11.025.
Hughes, M., Kaylor, S., Hayes, D., 2017. Patch-based forest change detection from Landsat time series. Forests 8, 166. https://doi.org/10.3390/f8050166.
Huntington, J.L., Hegewisch, K.C., Daudert, B., Morton, C.G., Abatzoglou, J.T., McEvoy, D.J., Erickson, T., 2017. Climate engine: cloud computing and visualization of climate and remote sensing data for advanced natural resource monitoring and process understanding. Bull. Am. Meteorol. Soc. 98, 2397–2409. https://doi.org/10.1175/BAMS-D-15-00324.1.
Kauth, R.J., Thomas, G.S., 1976. Tasselled Cap - a Graphic Description of the Spectral-Temporal Development of Agricultural Crops As Seen By Landsat. in: LARS Symposia. pp. 41–51.
Kennedy, R., Yang, Z., Gorelick, N., Braaten, J., Cavalcante, L., Cohen, W., Healey, S., 2018. Implementation of the LandTrendr Algorithm on Google Earth Engine. Remote Sens. 10, pp. 691– 691. doi:10.3390/RS10050691.
Kennedy, R.E., Yang, Z., Cohen, W.B., 2010. Detecting trends in forest disturbance and recovery using yearly Landsat time series: 1. LandTrendr - Temporal segmentation algorithms. Remote Sens. Environ. 114, 2897–2910. https://doi.org/10.1016/j.rse.2010.07.008.
Key, C.H., Benson, N., 1999. The Normalized Burn Ratio (NBR): a Landsat TM radiometric measure of burn severity, US Geological Survey Northern Rocky Mountain Science Center.
Lambin, E.F., 1999. Monitoring forest degradation in tropical regions by remote sensing : some methodological issues. Glob. Ecol. Biogeogr. 8, 191–198.
le Polain de Waroux, Y., Baumann, M., Gasparri, N.I., Gavier-Pizarro, G., Godar, J., Kuemmerle, T., Müller, R., Vázquez, F., Volante, J.N., Meyfroidt, P., 2018. Rents, actors, and the expansion of commodity frontiers in the Gran Chaco. Ann. Am. Assoc. Geogr. 108, 204–225. https://doi.org/10.1080/24694452.2017.1360761.
Leguizamón, A., 2014. Modifying Argentina: GM soy and socio-environmental change. Geoforum 53, 149–160. https://doi.org/10.1016/j.geoforum.2013.04.001.
Lyons, M.B., Keith, D.A., Phinn, S.R., Mason, T.J., Elith, J., 2018. A comparison of resampling methods for remote sensing classification and accuracy assessment. Remote Sens. Environ. 208, 145–153. https://doi.org/10.1016/j.rse.2018.02.026.
Macchi, L., Grau, H.R., 2012. Piospheres in the dry Chaco. Contrasting effects of livestock puestos on forest vegetation and bird communities. J. Arid Environ. 87, 176–187. https://doi.org/10.1016/j.jaridenv.2012.06.003.
Matricardi, E.A.T., Skole, D.L., Pedlowski, M.A., Chomentowski, W., Fernandes, L.C., 2010. Assessment of tropical forest degradation by selective logging and fire using Landsat imagery. Remote Sens. Environ. 114, 1117–1129. https://doi.org/10.1016/j.rse.2010.01.001.
Mckee, T.B., Doesken, N.J., Kleist, J., 1993. The relationship of drought frequency and duration to time scales. In: Proceeding Eighth Conf. Appl. Climatol. 17-22 January 1993, Anaheim, Calif. doi:citeulike-article-id:10490403.
Miles, L., Newton, A.C., DeFries, R.S., Ravilious, C., May, I., Blyth, S., Kapos, V., Gordon, J.E., 2006. A global overview of the conservation status of tropical dry forests. J. Biogeogr. 33, 491–505. https://doi.org/10.1111/j.1365-2699.2005.01424.x.
Minetti, J., 1999. Atlas Climático del Noroeste Argentino. Fundación Zon Caldenius, Tucuman, Argentina.
Morales-Barquero, L., Borrego, A., Skutsch, M., Kleinn, C., Healey, J.R., 2015. Identification and quantification of drivers of forest degradation in tropical dry forests: A case study in Western Mexico. Land Use Policy 49, 296–309. https://doi.org/10.1016/j.landusepol.2015.07.006.
Murdiyarso, D., Skutsch, M., Guariguata, M., Kanninen, M., Luttrell, C., Verweij, P., 2007. How do we measure and monitor forest degradation?, 1-1 Moving Ahead with REDD. https://doi.org/10.1002/tqem.3310060102.
Murphy, P.G., Lugo, A.E., 1986. Ecology of tropical dry forest. Annu. Rev. Ecol. Syst. 17, 67–88. https://doi.org/10.1146/annurev.es.17.110186.000435.
Olofsson, P., Foody, G.M., Herold, M., Stehman, S.V., Woodcock, C.E., Wulder, M.A., 2014. Good practices for estimating area and assessing accuracy of land change. Remote Sens. Environ. 148, 42–57. https://doi.org/10.1016/j.rse.2014.02.015.
Olson, D.M., Dinerstein, E., Wikramanayake, E.D., Burgess, N.D., Powell, G.V.N., Underwood, E.C., D'amico, J.A., Itoua, I., Strand, H.E., Morrison, J.C., Loucks, C.J., Allnutt, T.F., Ricketts, T.H., Kura, Y., Lamoreux, J.F., Wettengel, W.W., Hedao, P., Kassem, K.R., 2001. Terrestrial Ecoregions of the World: A New Map of Life on Earth. Bioscience 51, 933. https://doi.org/10.1641/0006-3568(2001)051[0933:TEOTWA]2.0.CO;2.
Pan, Y., Birdsey, R.A., Fang, J., Houghton, R., Kauppi, P.E., Kurz, W.A., Phillips, O.L., Shvidenko, A., Lewis, S.L., Canadell, J.G., Ciais, P., Jackson, R.B., Pacala, S.W., McGuire, A.D., Piao, S., Rautiainen, A., Sitch, S., Hayes, D., 2011. A large and persistent carbon sink in the world's forests. Science 333, 988–993. https://doi.org/10.1126/science.1201609.
Pearson, T.R.H., Brown, S., Murray, L., Sidman, G., 2017. Greenhouse gas emissions from tropical forest degradation: an underestimated source. Carbon Balance Manag. 12 https://doi.org/10.1186/s13021-017-0072-2.
Penalba, O., Rivera, J., 2015. Comparación de seis índices para el monitoreo de sequías meteorológicas en el sur de sudamérica. Meteorológica 40, 33–57.
Peri, P.L., Banegas, N., Gasparri, I., Carranza, C.H., Rossner, B., Pastur, G.M., Cavallero, L., López, D.R., Loto, D., Fernández, P., Powel, P., Ledesma, M., Pedraza, R., Albanesi, A., Bahamonde, H., Eclesia, R.P., Piñeiro, G., 2017. Carbon Sequestration in Temperate Silvopastoral Systems, Argentina. In: Integrating Landscapes: Agroforestry for Biodiversity Conservation and Food Sovereignty, pp. 453–478. doi: 10.1007/978-3-319-69371-2_19.
Piquer-Rodríguez, M., Butsic, V., Gärtner, P., Macchi, L., Baumann, M., Gavier Pizarro, G., Volante, J.N., Gasparri, I.N., Kuemmerle, T., 2018. Drivers of agricultural land-use change in the Argentine Pampas and Chaco regions. Appl. Geogr. 91, 111–122. https://doi.org/10.1016/j.apgeog.2018.01.004.
Piquer-Rodríguez, M., Torella, S., Gavier-Pizarro, G., Volante, J., Somma, D., Ginzburg, R., Kuemmerle, T., 2015. Effects of past and future land conversions on forest connectivity in the Argentine Chaco. Landsc. Ecol. 30, 817–833. https://doi.org/10.1007/s10980-014-0147-3.
Portillo-Quintero, C., Sánchez-Azofeifa, G.A., 2010. Extent and conservation of tropical dry forests in the Americas. Biol. Conserv. 143, 144–155. https://doi.org/10.1016/j.biocon.2009.09.020.
Powell, P.A., Nanni, A.S., Názaro, M.G., Loto, D., Torres, R., Gasparri, N.I., 2018. Characterization of forest carbon stocks at the landscape scale in the Argentine Dry Chaco. For. Ecol. Manage. 424, 21–27. https://doi.org/10.1016/j.foreco.2018.04.033.
Prado, D.E., 1993. What is the Gran Chaco vegetation in South America? I: A review. Contribution to the study of flora and vegetaion of the Chaco. V. Candollea 48, 145–172.
Rivera, J.A., Hinrichs, S., Marianetti, G., 2019. Using CHIRPS dataset to assess wet and dry conditions along the semiarid central-western Argentina. Adv. Meteorol. 2019 https://doi.org/10.1155/2019/8413964.
Romero-Muñoz, A., Benítez-López, A., Zurell, D., Baumann, M., Camino, M., Decarre, J., Castillo, H., Giordano, A.J., Gómez-Valencia, B., Levers, C., Noss, A.J., Quiroga, V., Thompson, J.J., Torres, R., Velilla, M., Weiler, A., Kuemmerle, T., 2020. Increasing synergistic effects of habitat destruction and hunting on mammals over three decades in the Gran Chaco. Ecography (Cop.) 43, 954–966. https://doi.org/10.1111/ecog.05053.
Romero-Muñoz, A., Torres, R., Noss, A.J., Giordano, A.J., Quiroga, V., Thompson, J.J., Baumann, M., Altrichter, M., McBride, R., Velilla, M., Arispe, R., Kuemmerle, T., 2019. Habitat loss and overhunting synergistically drive the extirpation of jaguars from the Gran Chaco. Divers. Distrib. 25, 176–190. https://doi.org/10.1111/ddi.12843.
Roy, D.P., Kovalskyy, V., Zhang, H.K., Vermote, E.F., Yan, L., Kumar, S.S., Egorov, A., 2016. Characterization of Landsat-7 to Landsat-8 reflective wavelength and normalized difference vegetation index continuity. Remote Sens. Environ. 185, 57–70. https://doi.org/10.1016/j.rse.2015.12.024.
Rozzi, R., 2012. Biocultural ethics: recovering the vital links between the inhabitants, their habits, and habitats. Environ. Ethics 34, 27–50. https://doi.org/10.5840/enviroethics20123414.
Rueda, C.V., Baldi, G., Gasparri, I., Jobbágy, E.G., 2015. Charcoal production in the Argentine Dry Chaco: where, how and who? Energy Sustain. Dev. 27, 46–53. https://doi.org/10.1016/j.esd.2015.04.006.
Sánchez-Azofeifa, G.A., Portillo-Quintero, C., 2011. Extent and drivers of change of neotropical seasonally dry tropical forests. In: Dirzo, R., Young, H.S., Mooney, H.A., Ceballos, G. (Eds.), Seasonally Dry Tropical Forests. Island Press/Center for Resource Economics, Washington, DC, pp. 45–57. https://doi.org/10.5822/978-1-61091-021-7_3.
Sánchez-Azofeifa, G.A., Quesada, M., Rodríguez, J.P., Nassar, J.M., Stoner, K.E., Castillo, A., Garvin, T., Zent, E.L., Calvo-Alvarado, J.C., Kalacska, M.E.R., Fajardo, L., Gamon, J.A., Cuevas-Reyes, P., 2005. Research priorities for neotropical dry forests. Biotropica 37, 477–485. https://doi.org/10.1046/j.0950-091x.2001.00153.x-i1.
Sasaki, N., Putz, F.E., 2009. Critical need for new definitions of "forest" and "forest degradation" in global climate change agreements. Conserv. Lett. 2, 226–232. https://doi.org/10.1111/j.1755-263X.2009.00067.x.
Saxena, R., Watson, L.T., Wynne, R.H., Brooks, E.B., Thomas, V.A., Zhiqiang, Y., Kennedy, R.E., 2018. Towards a polyalgorithm for land use change detection. ISPRS J. Photogramm. Remote Sens. 144, 217–234. https://doi.org/10.1016/j.isprsjprs.2018.07.002.
SAyDS, 2019. Nivel de referencia de emisiones forestales de la República Argentina. Secretaria de Ambiente y Desarrollo Sustentable República Argentina.

Schneibel, A., Stellmes, M., Röder, A., Frantz, D., Kowalski, B., Haß, E., Hill, J., 2017. Assessment of spatio-temporal changes of smallholder cultivation patterns in the Angolan Miombo belt using segmentation of Landsat time series. Remote Sens. Environ. 195, 118–129. https://doi.org/10.1016/j.rse.2017.04.012.

Schröder, J.M., Ávila Rodríguez, L.P., Günter, S., 2021. Research trends: tropical dry forests: the neglected research agenda? For. Policy Econ. 122, 102333 https://doi.org/10.1016/j.forpol.2020.102333.

Schultz, M., Clevers, J.G.P.W., Carter, S., Verbesselt, J., Avitabile, V., Quang, H.V., Herold, M., 2016. Performance of vegetation indices from Landsat time series in deforestation monitoring. Int. J. Appl. Earth Obs. Geoinf. 52, 318–327. https://doi.org/10.1016/j.jag.2016.06.020.

Semper-Pascual, A., Decarre, J., Baumann, M., Camino, M., Di Blanco, Y., Gómez-Valencia, B., Kuemmerle, T., 2020. Using occupancy models to assess the direct and indirect impacts of agricultural expansion on species' populations. Biodivers. Conserv. 1–20 https://doi.org/10.1007/s10531-020-02042-1.

Semper-Pascual, A., Macchi, L., Sabatini, F.M., Decarre, J., Baumann, M., Blendinger, P. G., Gómez-Valencia, B., Mastrangelo, M.E., Kuemmerle, T., 2018. Mapping extinction debt highlights conservation opportunities for birds and mammals in the South American Chaco. J. Appl. Ecol. 55, 1218–1229. https://doi.org/10.1111/1365-2664.13074.

Smith, V., Portillo-Quintero, C., Sanchez-Azofeifa, A., Hernandez-Stefanoni, J.L., 2019. Assessing the accuracy of detected breaks in Landsat time series as predictors of small scale deforestation in tropical dry forests of Mexico and Costa Rica. Remote Sens. Environ. 221, 707–721. https://doi.org/10.1016/j.rse.2018.12.020.

Souza, C.M., Roberts, D.A., Cochrane, M.A., 2005. Combining spectral and spatial information to map canopy damage from selective logging and forest fires. Remote Sens. Environ. 98, 329–343. https://doi.org/10.1016/j.rse.2005.07.013.

Stehman, S.V., 2013. Estimating area from an accuracy assessment error matrix. Remote Sens. Environ. 132, 202–211. https://doi.org/10.1016/j.rse.2013.01.016.

Torrella, S.A., Adámoli, J., 2005. Situación Ambiental de La Ecorregión Chaco Seco, La Situación Ambiental Argentina 2005.

Verbesselt, J., Hyndman, R., Newnham, G., Culvenor, D., 2010. Detecting trend and seasonal changes in satellite image time series. Remote Sens. Environ. 114, 106–115. https://doi.org/10.1016/j.rse.2009.08.014.

Wang, Y., Ziv, G., Adami, M., Mitchard, E., Batterman, S.A., Buermann, W., Schwantes Marimon, B., Marimon Junior, B.H., Matias Reis, S., Rodrigues, D., Galbraith, D., 2019. Mapping tropical disturbed forests using multi-decadal 30 m optical satellite imagery. Remote Sens. Environ. 221, 474–488. https://doi.org/10.1016/j.rse.2018.11.028.

Watson, J.E.M., Evans, T., Venter, O., Williams, B., Tulloch, A., Stewart, C., Thompson, I., Ray, J.C., Murray, K., Salazar, A., McAlpine, C., Potapov, P., Walston, J., Robinson, J.G., Painter, M., Wilkie, D., Filardi, C., Laurance, W.F., Houghton, R.A., Maxwell, S., Grantham, H., Samper, C., Wang, S., Laestadius, L., Runting, R.K., Silva-Chávez, G.A., Ervin, J., Lindenmayer, D., 2018. The exceptional value of intact forest ecosystems. Nat. Ecol. Evol. 2, 599–610. https://doi.org/10.1038/s41559-018-0490-x.

Woodcock, C.E., Loveland, T.R., Herold, M., Bauer, M.E., 2020. Transitioning from change detection to monitoring with remote sensing: a paradigm shift. Remote Sens. Environ. 238, 111558 https://doi.org/10.1016/j.rse.2019.111558.

Zak, M.R., Cabido, M., Cáceres, D., Díaz, S., 2008. What drives accelerated land cover change in central Argentina? Synergistic consequences of climatic, socioeconomic, and technological factors. Environ. Manage. 42, 181–189. https://doi.org/10.1007/s00267-008-9101-y.

Zak, M.R., Cabido, M., Hodgson, J.G., 2004. Do subtropical seasonal forests in the Gran Chaco, Argentina, have a future? Biol. Conserv. 120, 589–598. https://doi.org/10.1016/j.biocon.2004.03.034.

Zhu, Z., Woodcock, C.E., 2014. Continuous change detection and classification of land cover using all available Landsat data. Remote Sens. Environ. 144, 152–171. https://doi.org/10.1016/j.rse.2014.01.011.